Research Article | Vol. 25, No. 6 | 20 Mar 2017 | OPTICS EXPRESS 7084

Optics EXPRESS

Thulium doped LuAG ceramics for passively mode locked lasers

YICHENG WANG,[1] RUIJUN LAN,[2] XAVIER MATEOS,[1,3] JIANG LI,[4] CHAOYU LI,[4] SOILE SUOMALAINEN,[5] ANTTI HÄRKÖNEN,[5] MIRCEA GUINA,[5] VALENTIN PETROV,[1] AND UWE GRIEBNER[1,*]

[1]*Max Born Institute for Nonlinear Optics and Short Pulse Spectroscopy, Max-Born-Str. 2a, Berlin 12489, Germany*
[2]*School of Opto-Electronic Information Science and Technology, Yantai University, Yantai 264005, China*
[3]*Física i Cristal·lografia de Materials i Nanomaterials, Universitat Rovira i Virgili, Campus Sescelades, c/ Marcel·lí Domingo, s/n., Tarragona, E-43007 Spain*
[4]*Key Laboratory of Transparent and Opto-Functional Inorganic Materials, CAS Shanghai Institute of Ceramics, Chinese Academy of Sciences, 1295 Dingxi Road, Shanghai 200050, China*
[5]*Optoelectronics Research Centre, Tampere University of Technology, PO Box 692, Tampere 33101, Finland*
**griebner@mbi-berlin.de*

Abstract: Passive mode-locking of a thulium doped $Lu_3Al_5O_{12}$ ceramic laser is demonstrated at 2022 nm. By applying different near surface GaSb-based saturable absorber mirrors, stable self-starting mode-locked operation with pulse durations between 2 and 4 picoseconds was achieved at a repetition rate of 92 MHz. The SESAM mode-locked Tm:LuAG ceramic laser exhibits an excellent stability with a fundamental beat note extinction ratio of 80 dB above the noise level. Furthermore, spectroscopic properties of Tm:LuAG ceramics at room temperature are presented.

OCIS codes: (140.4050) Mode-locked lasers; (140.3070) Infrared and far-infrared lasers; (160.3380) Laser materials.

References and links

1. K. Scholle, S. Lamrini, P. Koopmann, and P. Fuhrberg, "2 µm laser sources and their possible applications," in *Frontiers in Guided Wave Optics and Optoelectronics*, Bishnu Pal, ed. (InTech, 2010), pp. 471–500.
2. V. Petrov, "Frequency down-conversion of solid-state laser sources to the mid-infrared spectral range using non-oxide nonlinear crystals," Prog. Quantum Electron. **42**, 1–106 (2015).
3. A. Dergachev, "High-energy, kHz, picosecond, 2-µm laser pump source for mid-IR nonlinear optical devices," Proc. SPIE **8599**, 85990B (2013).
4. R. Targ, B. C. Steakley, J. G. Hawley, L. L. Ames, P. Forney, D. Swanson, R. Stone, R. G. Otto, V. Zarifis, P. Brockman, R. S. Calloway, S. H. Klein, and P. A. Robinson, "Coherent lidar airborne wind sensor II: flight-test results at 2 and 10 vm," Appl. Opt. **35**(36), 7117–7127 (1996).
5. T. M. Taczak and D. K. Killinger, "Development of a tunable, narrow-linewidth, cw 2.066-µm Ho:YLF laser for remote sensing of atmospheric CO_2 and H_2O," Appl. Opt. **37**(36), 8460–8476 (1998).
6. U. N. Singh, B. M. Walsh, J. Yu, M. Petros, M. J. Kavaya, T. F. Refaat, and N. P. Barnes, "Twenty years of Tm:Ho:YLF and LuLiF laser development for global wind and carbon dioxide active remote sensing," Opt. Mater. Express **5**(4), 827–837 (2015).
7. Q. Wang, J. Geng, T. Luo, and S. Jiang, "Mode-locked 2 mum laser with highly thulium-doped silicate fiber," Opt. Lett. **34**(23), 3616–3618 (2009).
8. M. Zhang, E. J. R. Kelleher, F. Torrisi, Z. Sun, T. Hasan, D. Popa, F. Wang, A. C. Ferrari, S. V. Popov, and J. R. Taylor, "Tm-doped fiber laser mode-locked by graphene-polymer composite," Opt. Express **20**(22), 25077–25084 (2012).
9. A. Schmidt, S. Y. Choi, D. Yeom, F. Rotermund, X. Mateos, M. Segura, F. Díaz, V. Petrov, and U. Griebner, "Femtosecond pulses near 2 µm from a Tm:KLuW laser mode-locked by a single-walled carbon nanotube saturable absorber," Appl. Phys. Express **5**(9), 092704 (2012).
10. A. Ikesue, K. Kamata, and K. Yoshida, "Synthesis of Nd^{3+}, Cr^{3+}-codoped YAG ceramics for high-efficiency solid-state lasers," J. Am. Ceram. Soc. **78**(9), 2545–2547 (1995).

#285270 https://doi.org/10.1364/OE.25.007084
Journal © 2017 Received 19 Jan 2017; revised 8 Mar 2017; accepted 10 Mar 2017; published 17 Mar 2017

Optics EXPRESS

11. A. Ikesue, Y. L. Aung, T. Taira, T. Kamimura, K. Yoshida, and G. L. Messing, "Progress in ceramic lasers," Annu. Rev. Mater. Res. **36**(1), 397–429 (2006).
12. A. Ikesue and Y. L. Aung, "Ceramic laser materials," Nat. Photonics **2**(12), 721–727 (2008).
13. J. Li, Y. Pan, Y. Zeng, W. Liu, B. Jiang, and J. Guo, "The history, development, and future prospects for laser ceramics: a review," Int. J. Refract. Met. Hard Mater. **39**, 44–52 (2013).
14. W. Zhang, Y. Pan, J. Zhou, W. Liu, J. Li, B. Jiang, X. Cheng, and J. Xu, "Diode-pumped Tm:YAG ceramic laser," J. Am. Ceram. Soc. **92**(10), 2434–2437 (2009).
15. Q. Ma, Y. Bo, N. Zong, Y. Pan, Q. Peng, D. Cui, and Z.-Y. Xu, "Light scattering and 2-μm laser performance of Tm:YAG ceramic," Opt. Commun. **284**(6), 1645–1647 (2011).
16. W. L. Gao, J. Ma, G. Q. Xie, J. Zhang, D. W. Luo, H. Yang, D. Y. Tang, J. Ma, P. Yuan, and L. J. Qian, "Highly efficient 2 μm Tm:YAG ceramic laser," Opt. Lett. **37**(6), 1076–1078 (2012).
17. S. Zhang, X. Wang, W. Kong, Q. Yang, J. Xu, B. Jiang, and Y. Pan, "Efficient Q-switched Tm:YAG ceramic slab laser pumped by a 792 nm fiber laser," Opt. Commun. **286**, 288–290 (2013).
18. Y. Zou, Z. Wei, Q. Wang, M. Zhan, D. Li, Z. Zhang, J. Zhang, and D. Tang, "High-efficiency diode-pumped Tm:YAG ceramic laser," Opt. Mater. **35**(4), 804–806 (2013).
19. E. D. Filer, N. P. Barnes, and C. A. Morrison, "Theoretical temperature dependent branching ratios and laser thresholds of the $^3F_4$ to $^3H_6$ levels of Tm in ten garnets," in Advanced Solid State Lasers, G. Dubé, L. Chase, eds., Vol. 10 of OSA Proceedings Series (OSA, Washington, D.C., 1993), pp. 189–200.
20. N. P. Barnes, M. G. Jani, and R. L. Hutcheson, "Diode-pumped, room-temperature Tm:LuAG laser," Appl. Opt. **34**(21), 4290–4294 (1995).
21. K. Scholle, E. Heumann, and G. Huber, "Single mode Tm and Tm,Ho:LuAG lasers for LIDAR applications," Laser Phys. Lett. **1**(6), 285–290 (2004).
22. C. Wu, Y. Ju, Y. Li, Z. Wang, and Y. Wang, "Diode-pumped Tm:LuAG laser at room temperature," Chin. Opt. Lett. **6**(6), 415–416 (2008).
23. T. Feng, K. Yang, S. Zhao, J. Zhao, W. Qiao, T. Li, L. Zheng, J. Xu, Q. Wang, X. Xu, L. Su, and Y. Wang, "Efficient CW dual-wavelength and passively Q-switched Tm:LuAG lasers," IEEE Photonics Technol. Lett. **27**, 7–10 (2015).
24. T. Feng, K. Yang, J. Zhao, S. Zhao, W. Qiao, T. Li, T. Dekorsy, J. He, L. Zheng, Q. Wang, X. Xu, L. Su, and J. Xu, "1.21 W passively mode-locked Tm:LuAG laser," Opt. Express **23**(9), 11819–11825 (2015).
25. A. Gluth, Y. Wang, V. Petrov, J. Paajaste, S. Suomalainen, A. Härkönen, M. Guina, G. Steinmeyer, X. Mateos, S. Veronesi, M. Tonelli, J. Li, Y. Pan, J. Guo, and U. Griebner, "GaSb-based SESAM mode-locked Tm:YAG ceramic laser at 2 μm," Opt. Express **23**(2), 1361–1369 (2015).
26. Y. Wang, R. Lan, X. Mateos, J. Li, C. Hu, C. Li, S. Suomalainen, A. Härkönen, M. Guina, V. Petrov, and U. Griebner, "Broadly tunable mode-locked Ho:YAG ceramic laser around 2.1 μm," Opt. Express **24**(16), 18003–18012 (2016).
27. U. Keller, K. J. Weingarten, F. X. Kärtner, D. Kopf, B. Braun, I. D. Jung, R. Fluck, C. Hönninger, N. Matuschek, and J. Aus der Au, "Semiconductor saturable absorber mirrors (SESAM's) for femtosecond to nanosecond pulse generation in solid-state lasers," IEEE J. Sel. Top. Quantum Electron. **2**(3), 435–453 (1996).
28. J. Paajaste, S. Suomalainen, A. Härkönen, U. Griebner, G. Steinmeyer, and M. Guina, "Absorption recovery dynamics in 2 μm GaSb-based SESAMs," J. Phys. D Appl. Phys. **47**(6), 065102 (2014).
29. J. Paajaste, S. Suomalainen, R. Koskinen, A. Härkönen, G. Steinmeyer, and M. Guina, "GaSb-based semiconductor saturable absorber mirrors for mode-locking 2 μm semiconductor disk lasers," Phys. Status Solidi **9**(2), 294–297 (2012).
30. Y. Fu, J. Li, C. Wang, T. Xie, W. Li, L. Wu, and Y. Pan, "Fabrication and properties of highly transparent Yb:LuAG ceramics," J. Alloys Compd. **664**, 595–601 (2016).
31. Y. Wang, G. Xie, X. Xu, J. Di, Z. Qin, S. Suomalainen, M. Guina, A. Härkönen, A. Agnesi, U. Griebner, X. Mateos, P. Loiko, and V. Petrov, "SESAM mode-locked Tm:CALGO laser at 2 μm," Opt. Mater. Express **6**(1), 131–136 (2016).

1. Introduction

Ultrashort pulse lasers around 2 μm have been drawing great attention since they are applied in various fields including physics, chemistry and biology [1]. Such ultrafast 2 μm lasers are in particular used as pump and seed sources in optical parametric amplifiers for the mid-IR spectral range and for global wind and carbon dioxide active remote sensing [2–6]. The thulium ion (Tm^{3+}) doped in different host materials including crystals and glasses, is an attractive solution for building ultrashort pulse laser sources around 2 μm [7–9]. Due to the cross relaxation process between the thulium ions in the host the quantum efficiency can be doubled at higher doping levels. Such lasers can also benefit from the availability of long time proved and commercially available 800 nm laser diodes as pump sources.

Among the corresponding host materials, laser grade transparent ceramics exhibit a number of favorable properties such as the generally simpler manufacturing procedure compared to the growth of single crystals, or the almost unlimited dimensions, as well as

Optics EXPRESS

other aspects like higher doping concentrations, and simplified shaping and processing [10–13]. Successful demonstrations of ceramic lasers have been restricted so far to isotropic materials, such as garnets and the cubic sesquioxides (e.g. LuAG, YAG, Lu_2O_3, Sc_2O_3, Y_2O_3). With regard to Tm-doping, YAG ceramics is considered as the most promising host due to its robust thermal performance as well as excellent optical properties. During the last several years, the continuous-wave (CW) laser performance of Tm:YAG ceramics was significantly improved, and output powers of several Watts were obtained with slope efficiencies up to 65% [14–18]. The Y and Lu ions have similar radii and masses. Hence, the incorporation of Lu-ions instead of Y-ions in the garnet host should result in a similar laser performance with Tm-doping. Moreover, theoretical and experiment studies indicated that LuAG is a more suitable host for Tm^{3+} compared to YAG [19, 20]. In addition, the free running emission wavelength of Tm:LuAG is 2022 nm, e.g. ~10 nm red-shifted compared to Tm:YAG, which fits much better one of the atmospheric optical transmission windows. This property attracted the attention to Tm:LuAG for LIDAR applications [21]. Tm:LuAG single crystals have already shown an exciting performance for both CW and pulsed laser operation, such as Q-switching and mode locking. A CW output power of 4.9 W and maximum slope efficiency of up to 49% were demonstrated [22, 23]. By applying GaAs-based semiconductor saturable absorber mirrors (SESAMs), a Tm:LuAG crystal laser delivered 38 ps pulses with 1.2 W output power [24]. From our experience with mode-locked Tm- and Ho-doped YAG ceramic lasers, we believe there is still great potential for improving the performance in terms of pulse duration of mode-locked Tm:LuAG oscillators employing laser ceramics [25, 26].

SESAMs are commonly employed as saturable absorbers for passive mode-locking of various lasers [27], including a large number of Tm-, Tm,Ho- and Ho-based bulk lasers emitting around 2 µm [4–9]. However, despite the recent progress of SESAM technology around 2 µm, they have not reached the maturity level of those utilized in the spectral range around 1 µm, yet. In the 2 µm spectral range, GaSb-based quantum well (QW) structures have proven their suitability as saturable absorbers for mode-locking of Tm- and Ho-doped laser materials. Post-processing and near surface quantum well designs were investigated for such types of SESAMs to accelerate the relaxation process [28, 29]. The nonlinear properties of GaSb-based SESAMs exhibiting "classical" and near surface designs have been studied revealing a surprisingly fast absorption recovery time of a few picoseconds which is rather independent of growth temperature or strain in the QWs [28].

In this paper the first laser operation of a Tm:LuAG ceramic laser is demonstrated. Wavelength tuning in the CW regime is studied as well as passive mode-locking. Employing near surface GaSb-based SESAMs, the Tm:LuAG ceramic laser delivered record short pulse durations of a few picoseconds.

2. Tm:LuAG ceramics and semiconductor saturable absorber

A 4 at.% Tm-doped LuAG ceramic was obtained by the solid-state reactive sintering method using high-purity powders of Lu_2O_3, α-Al_2O_3 and Tm_2O_3 as starting materials similar to the procedure reported in [30]. A 3 mm long highly transparent active element with an aperture of ~5 × 5 mm^2 was prepared for lasing operation. No coating was applied for the optically polished input and output faces. For cooling the ceramic was placed in a copper holder, wrapped in Indium foil for good thermal contact with all the four lateral faces.

In the literature, spectroscopic data are only available for Tm:LuAG single crystals [20–22]. Here we present the laser-relevant spectroscopic characterization of Tm:LuAG ceramics. The largest absorption cross sections of the $^3H_6 \rightarrow {}^3H_4$ Tm^{3+} transition amount to 4.27 × 10^{-21} cm^2 at 783 nm and 4.17 × 10^{-21} cm^2 at 787 nm. We derived an emission cross section σ_e of the $^3F_4 \rightarrow {}^3H_6$ Tm^{3+} transition from the absorption cross section σ_a according to the McCumber theory. Both cross sections of the $^3F_4 \leftrightarrow {}^3H_6$ transition are shown in Fig. 1(a) for the wavelengths range 1800 to 2100 nm. In order to estimate the potential emission wavelengths around 2 µm of the Tm:LuAG ceramics, the gain cross section, $\sigma_{gain} = \beta\sigma_e - (1-\beta)\sigma_a$, is

Optics EXPRESS

calculated for several values of the population inversion parameter β and presented in Fig. 1(b). β is the ratio of the number of excited Tm^{3+}-ions in the $^3F_4$ manifold to the total Tm^{3+}-ion density. For the $^3F_4 \rightarrow {}^3H_6$ Tm^{3+} transition, the Tm:LuAG ceramics cross sections are very similar to those of their single crystal counterpart [21]. The maximum emission cross section of the ceramic for the laser transition from the $^3F_4$ level to the ground state is 1.51×10^{-21} cm^2 at 2023 nm and the linewidth is 30 nm (FWHM). The maximum σ_e is only slightly lower compared to Tm:LuAG single crystals: $\sigma_e = 1.66 \times 10^{-21}$ cm^2 [21]. A relaxation time of the $^3F_4$ emission for the 4 at.% Tm:LuAG ceramics of 10 ms was obtained at room temperature and is in good agreement with the lifetime reported for single crystals [21].

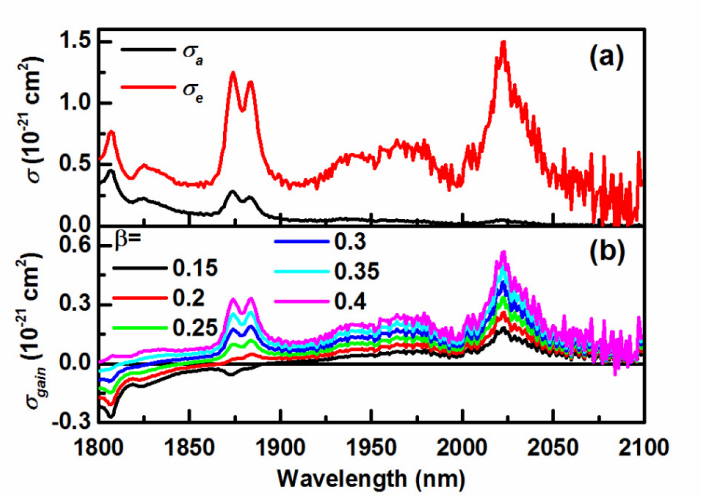

Fig. 1. Spectroscopic properties of Tm-doped LuAG ceramics in the 2-µm region. (a) Absorption σ_a and emission σ_e cross section of the $^3F_4 \leftrightarrow {}^3H_6$ transition. (b) Gain cross section σ_{gain} for different inversion rates β.

The applied SESAMs were characterized with respect to their relaxation time τ_2 only recently. We studied GaSb-based SESAMs with a low number of QWs [28, 29]. The absorber region contains one or two InGaSb QWs, emitting at 2050 nm, embedded in GaSb. On top of the <10 nm thin cap layer an antireflection coating is deposited resulting in an anti-resonant SESAM design at the operating wavelength of 2 µm. In this way acceleration of the carrier recombination via surface recombination occurs, resulting in relaxation times <5 ps at 2 µm for the three SESAMs applied [28].

3. Experimental set-up

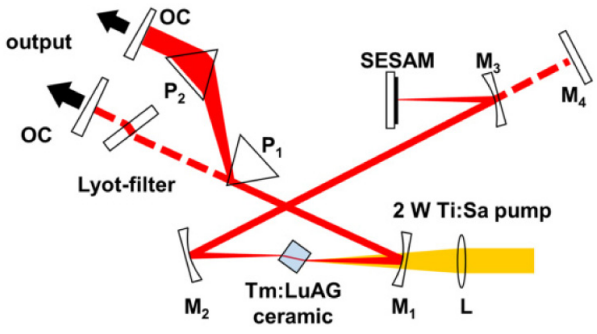

Fig. 2. Scheme of the Tm:LuAG ceramic laser (L: lens; M_1-M_4: mirrors (total reflectors); P_1-P_2: MgF_2 prisms; OC: output coupler).

Optics EXPRESS

A classical X-shaped cavity was employed for the laser experiments as shown in Fig. 2. The Tm:LuAG ceramic sample was placed at Brewster angle between two dichroic folding mirrors M_1 and M_2 (radius of curvature, RoC: −100 mm) with a separation of ~104 mm. For CW operation, the cavity was completed by a plane high reflecting end mirror M_4 and a wedged output coupler (OC). Additionally, wavelength tuning was performed by placing a birefringence filter at Brewster angel close to the OC.

For mode-locked operation, M_3 (RoC: −150 mm) was employed as a folding mirror to create a second intracavity beam waist with radius of ~100 µm at the position of the SESAM. In the other arm of the cavity, two MgF_2 prisms P_1 and P_2 were inserted for dispersion management. The total cavity length including the prism path amounted to about 1.62 m.

A CW titanium-sapphire laser was used as pump source delivering up to 2.1 W output power. The wavelength was tuned to the absorption maximum at 787 nm of the Tm-doped ceramics. The pump focus achieved by a 70 mm lens ensured a good overlap with the designed cavity laser mode with a radius of 36 µm.

4. Results and discussion

Initially the CW laser regime was investigated using the 4-mirror cavity scheme described above. The single-pass pumped Tm:LuAG ceramic has an average absorption of 71 ± 2% in the lasing state. No roll-off in the input-output dependence was observed during laser operation which is an indication of the high quality of the ceramic. By applying different output coupler (OC) transmissions, the slope efficiencies varied from 42% (1.5% OC) to 61% (5.0% OC) as shown in Fig. 3(a). The maximum output power amounted to 830 mW (5.0% OC) and the emission wavelength for all OCs was 2022 nm. Introducing the birefringence filter, a 3 mm thick quartz plate with the optical axis 60° to the surface, wavelength tuning of the Tm:LuAG ceramic was achieved as depicted in Fig. 3(b). The Tm:LuAG laser covers a wavelength tuning range of 280 nm (at 0-level) from 1808 to 2088 nm using the 1.5% OC and 15 nm narrower with the 3.0% OC, from 1808 to 2073 nm.

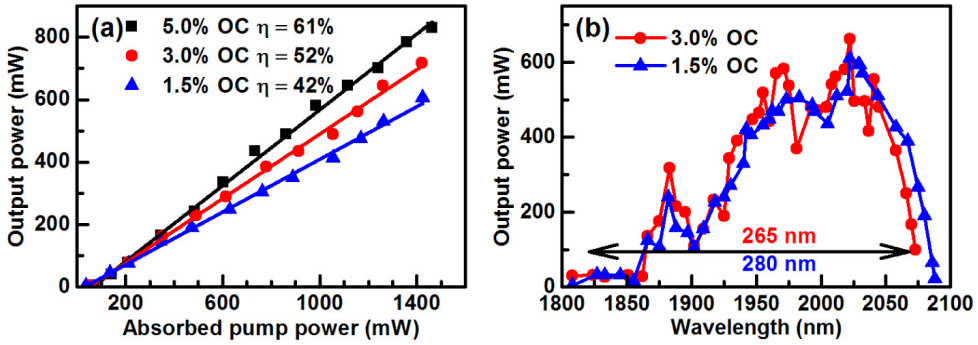

Fig. 3. Performance of the CW Tm:LuAG ceramic laser: (a) Output power versus absorbed pump power for different OCs. (b) Wavelength tuning at maximum pump power.

For mode-locking, three SESAMs with different number of quantum wells and thickness of the cap layer were tested. The SESAM parameters are listed in Table 1. The cavity was modified to the configuration for mode-locking, implementing the SESAM. The transmission of the OC had to be chosen >2.0% because otherwise a strong tendency of SESAM damage was observed even before mode-locking started. Increasing the mode size on the SESAM to potentially prevent its damage for OC transmissions <2.0% was not possible because of the available folding resonator mirrors. With the largest RoC of −150 mm, a maximum waist size at the SESAM position of ~110 µm could be realized. Thus 3.0% OC was applied to reduce the intracavity power and self-starting CW mode-locked laser operation was achieved easily without damage of the SESAMs. Depending on the SESAM parameters the mode-locked

Optics EXPRESS

laser undergoes different operation regimes in the applied pump power range (CW, Q-switched ML, CW-ML), as shown in Fig. 4(a). The corresponding parameters for the CW-ML regime are also included in Table 1.

Stable CW-ML operation was achieved with all three SESAMs. Using SESAM no. 1, a maximum average output power of 119 mW was reached. The CW-ML regime started from an absorbed power ~600 mW, with a slope efficiency of 14%. The corresponding non-collinear autocorrelation function (ACF) and optical spectrum are presented in Fig. 4(b). A pulse duration of τ = 3.8 ps at full width at half maximum (FWHM) is derived from the measured ACF under the assumption of a sech^2-pulse shape. The measured optical spectrum exhibited a FWHM of 2.3 nm at 2022 nm corresponding to a time bandwidth product (TBP) of 0.64. The ultimate stability was achieved by adding negative dispersion by introducing the prisms producing an intracavity round trip group delay dispersion (GDD) of –2021 fs^2 (prism separation: 21 cm). However, the prisms had no pulse shortening effect. In addition, a satellite was observed at 16 ps separation with an amplitude of only 2% of the main pulse.

Table 1. SESAM parameters and CW mode-locking results of the Tm:LuAG ceramic laser (3.0% OC).

SESAM	No. of QWs	Cap thickness (nm)	τ_2 (ps)	τ (ps)	TBP	F_{th} (μJ/cm^2)	P_{out} (mW)
no. 1	1	10	1.7	3.8	0.64	138	119
no. 2	1	5	1.7	2.9	0.55	503	270
no. 3	2	5	4.1	2.7	0.40	235	232

τ_2 – recovery time SESAM, slow component, τ – laser pulse duration, TBP – time bandwidth product, F_{th} – average fluence on the SESAM at the ML threshold, P_{out} – maximum average output power in the CW-ML regime.

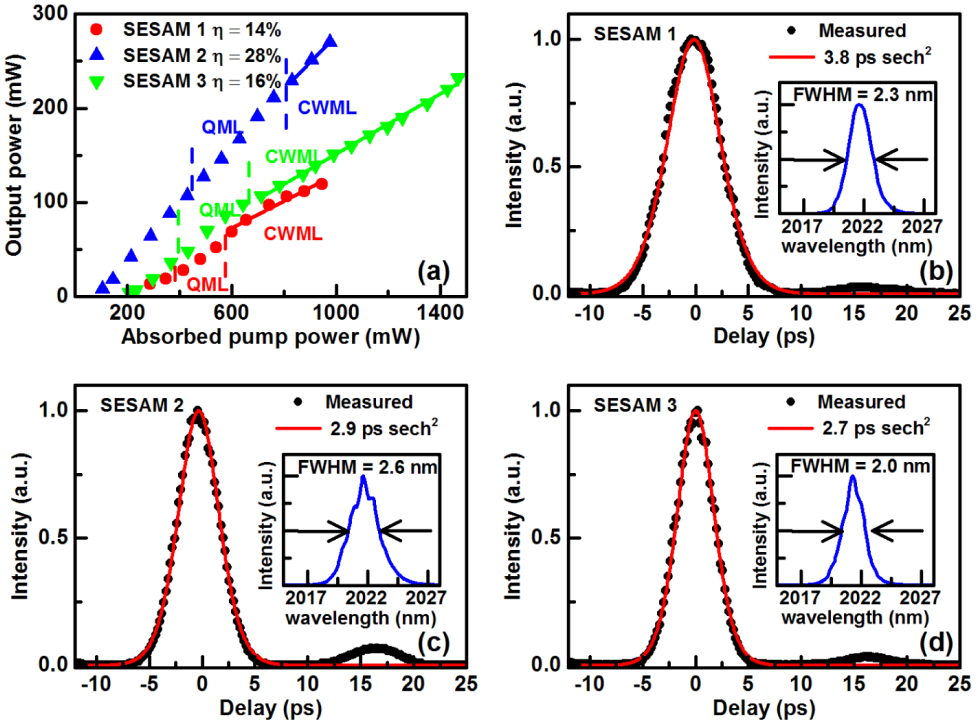

Fig. 4. Mode-locked Tm:LuAG ceramic laser. (a) Output power versus absorbed pump power for the different GaSb-based SESAMs (3% OC). (b)-(c) Autocorrelation functions and optical spectra (insets) of the shortest generated pulse at maximum average output power for the three different SESAMs.

Optics EXPRESS

Best performance with respect to average output power (270 mW) and slope efficiency (28%) was obtained with SESAM no. 2. However compared to SESAM no. 1 the CW-ML operation started at a rather high intracavity average fluence on the SESAM of F_{th} = 503 μJ/cm^2 and the stability range was narrower in terms of absorbed pump power [Fig. 4(a)]. The pulses were shorter, τ = 2.9 ps, compared to SESAM no. 1 but the amplitude of the satellite increased to about 7% of the main pulse at the same separation [Fig. 4(c)]. This led to observable modulation in the spectrum. The corresponding TBP of 0.55 is slightly closer to the TBP limit compared to SESAM no. 1.

The performance of SESAM no. 3 was superior in terms of the CW-ML operation range, extending from 700 mW up to the maximum pump power applied [Fig. 4(a)]. The pulses were as short as 2.7 ps (average output power: 232 mW) while the satellite amplitude was about 3% of the main pulse. This is illustrated in Fig. 4(d) together with the spectral modulation (inset). Here the corresponding TBP is the best and amounts to 0.40.

For SESAM no. 1 and no. 2 the fundamental mode-locking turns in a multi-pulsing regime for an absorbed pump power of >1 W which is connected with damaging [Fig. 4(a)]. In all cases, the satellite separation from the main pulse was exactly 16 ps, which closely matches with the roundtrip time in the SESAM's GaSb substrate. In other words, a part of the pulse energy, incident upon the SESAM, is transmitted through the DBR and reflected back from the back surface of the GaSb substrate, leading to formation of the satellite pulse. This spurious Fabry–Pérot (FP) effect is also confirmed by the modulation of the emission spectra in Fig. 4 ($\Delta\lambda_{mod}$ = 0.8 nm), which correlates with the free-spectral range of the ~520 μm thick GaSb substrate. We are convinced that the detected FP in the SESAM structure has no bandwidth-limiting effects for the mode-locked operation of the Tm:LuAG oscillator. We achieved sub-ps pulses with >9 nm bandwidth (FWHM) at 2020 nm with Tm:CALGO as active medium using a similar SESAM (same FP "sub-structure") [31]. It should be noticed that, the FP effect, can be easily suppressed by adding a few more layer pairs to the DBR and/or by further roughening the SESAMs back surface.

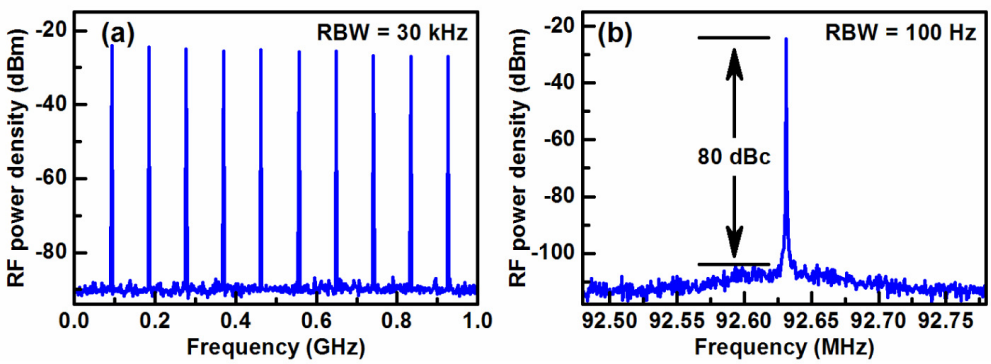

Fig. 5. Radio frequency spectra of the mode-locked Tm:LuAG ceramic laser using SESAM no. 3: (a) 1.0 GHz wide-span, (b) fundamental beat note (RBW: resolution bandwidth).

The stability of the mode-locked Tm:LuAG ceramic laser was characterized by the measurement of the radio frequency (RF) spectra and the results for SESAM no. 3 are shown in Fig. 5. The narrow band fundamental beat note was centered near 92.7 MHz with a high extinction ratio of 80 dB above noise level [Fig. 5(b)]. The RF spectra indicate a stable and clean CW mode-locking without Q-switching instabilities. This holds also when operating the laser in the CW-ML mode using SESAMs no. 1 and no. 2, with similar extinction ratios around 80 dB above noise level.

Optics EXPRESS

5. Conclusion

Thulium doped LuAG ceramics has been studied in CW and passively mode-locked lasers. The CW laser was characterized by a high slope efficiency of up to 61% and a total wavelength tuning range of 280 nm. Using GaSb-based SESAMs, the Tm:LuAG ceramic laser delivered pulses as short as 2.7 ps with an excellent stability. The stable self-starting mode-locked performance is evidenced by the extinction ratio of 80 dB above carrier of the first beat note in the RF spectrum. It crucially depends on the applied anti-resonant GaSb-based SESAMs exhibiting recovery times <5 ps. Compared to the so far only report on Tm:LuAG crystal laser mode-locked by a SESAM, one order of magnitude shorter pulses and two orders of magnitude better pulse contrast are achieved [25]. With respect to the previously reported performance of a mode-locked Tm:YAG ceramic laser, higher efficiency and output power are demonstrated at comparable pulse characteristics [26]. The exploitation of the great potential of Tm:LuAG ceramics for ultrashort pulse generation in the 2 μm spectral range will be the focus of further studies.

Funding

National Natural Science Foundation of China (NSFC) (No. 61405171); and the Key Research project of the Frontier Science of the Chinese Academy of Sciences (No. QYZDB-SSW-JSC022).